Technical University of Denmark

DTU

Influence of surface pretreatment in resistance spot welding of aluminum AA1050

Al Naimi, Ihsan K.; Al Saadi, Moneer H.; Daws, Kasim M.; Bay, Niels Oluf

DTU Library
Technical Information Center of Denmark

Influence of surface pretreatment in resistance spot welding of aluminum AA1050

Ihsan K. Al Naimi, Moneer H. Al Saadi, Kasim M. Daws & Niels Bay

Taylor & Francis
Taylor & Francis Group

Influence of surface pretreatment in resistance spot welding of aluminum AA1050

Ihsan K. Al Naimi[a]*, Moneer H. Al Saadi[b], Kasim M. Daws[a] and Niels Bay[c]

[a]Mechanical Department, College of Engineering, Baghdad University, Baghdad, Iraq; [b]Welding Department, University of Kerbala, Baghdad, Iraq; [c]Department of Mechanical Engineering, Technical University of Denmark, Lyngby, Denmark

Resistance spot welding (RSW) of aluminum alloys implies a major problem of inconsistent quality from weld to weld due to problems of varying thickness of the oxide layer. The high resistivity of oxide layer causes strong heat development, which has significant influence on electrode life and weld quality. An experimental study of the influence of pretreatment on weld quality in RSW of AA1050 sheets with three thicknesses, comparing welding of as-received sheet with pretreated sheet by either pickling in NaOH or glass-blasting were investigated. Different weld settings were applied with low-, medium-, and high-energy inputs. The as-received sheet showed higher electrical contact resistance because of thicker oxide layer. Lower values were noticed with pickled surfaces, whereas the lowest electrical contact resistance was obtained when glass blasting, resulting in the roughest surface topography, which facilitated breakdown the oxide layer. Highest strength and smaller scatter in strength were obtained by pickling in NaOH.

Keywords: resistance spot welding; contact resistance; oxide film; surface pretreatment

1. Introduction

The increasing demands for energy savings have implied special focus in automotive industry on lighter vehicles production, among other solutions by introducing skin panels of aluminum instead of steel. Weight savings up to 46% are reported (Wheeler, Sheasby, & Kewley, 1987), and furthermore resistance to corrosion is improved.

Resistance spot welding (RSW) is the most dominant process in sheet metal joining, particularly in automotive industry due to low cost, high productivity, flexibility, easy automation and maintenance, and minimum requirements for skilled labor (Brown, Newton, & Boomer, 1995; Cho, Li, & Hu, 2006; Spinella, Brockenbrough, & Fridy, 2005). The process is also widely applied in other industries of sheet product manufacturing, e.g. other transportation industries and in production of kitchen utensils.

It should, however, be emphasized that RSW of aluminum is more problematic than steel due to higher electrical and thermal conductivity, higher coefficient of expansion, lower melting temperature, and an oxide layer, which has high electrical resistance and high melting temperature (2050 °C). The latter together with the fact that the effective contact resistance grows considerably as the oxide film grows implies large scatter in

---

*Corresponding author. Email: ihsan_kad@yahoo.com

quality of RSW aluminum sheets, which therefore require close production control (Boomer, Hunter, & Castle, 2003; Kim, Park, Hwang, & Kang, 2009; Mathers, 2002).

The high thermal and electrical conductivity of aluminum require 2–3 times higher current and shorter weld time, typically 25% of that used to spot weld steel. Accurate control and synchronization of current and electrode force is required due to the narrow weld temperature range (*Resistance Welding Manual*, 2003). The problems are especially pronounced when welding unalloyed aluminum AA 1XXX.

Aluminum is highly reactive to oxygen, and after removal of the oxide layer by mechanical or chemical means, a new oxide layer will immediately form on its surface in normal atmosphere. The layer is beneficial as it protects the base metal from corrosion, but creates problems in connection with resistance welding, where it causes severe electrode degradation and scatter in weld quality due to (Han, Thornton, Boomer, & Shergold, 2010; Patrick, Auhl, & Sun, 1984; Sun, 1982). Spot welding in aluminum AA1050 is less stable than in alloyed aluminum, and the electrodes will stick to the sheet after 50 welds because of the oxide film problems (Pedersen, 2010). Contributions to the contact resistance comes from the oxide layer as well as the contaminant film, which may include dirt, lubricant, chemicals, and water vapor (Rashid, 2011; Sun, 2003). Even though maintenance of uniform surface conditions is taken carefully into consideration, the electrical contact resistance will vary from weld to weld implying inconsistent weld quality.

Contact resistance was experimentally investigated by Song, Zhang, and Bay (2005) using a Gleeble system. They showed that interface normal pressure had significant but decreasing influence on the contact resistance with increasing normal pressure, whereas the influence of temperature was less pronounced as pressure increased. Surface roughness together with elastic–plastic properties of the materials also influences the electrical contact resistance (Dzekster & Ismailov, 1990; Zheng, Shan, Hu, & Luo, 2006). Crinon and Evans (1998) showed that the effect of the oxide film is greatest for specimens with the smoothest surface.

Expulsion during RSW may either occur at the faying surfaces or the electrode/workpiece interfaces. The latter may severely affect surface quality and electrode life. The risk of expulsion is especially high in spot welding of aluminum due to the very dynamic and unstable character of the process, related to the requirements of high current and short welding time as compared to welding steels (Mathers, 2002; Senkara, Zhang, & Hu, 2004; Zhang & Senkara, 2012).

A large number of investigations in the literature deal with the influence of surface preparation on RSW of aluminum sheets. Rönnhult, Rilby, and Olefjord (1980) studied the weldability of aluminum alloy AA5252, both as-received and after etching in NaOH and oxalic acid, and proved that removing the oxide layer led to a significant improvement in weld quality. Etched, mill finish, and pretreated/lubricated AA5754 surfaces were examined by Thornton, Newton, Keay, Sheasby, and Evans (1997), they suggested that etched surfaces that had a thin and uniform oxide layer, gave the most consistent surface resistance and weld strength, which was in good agreement with other studies by Pickering and Hart (1994) and Li, Hao, Zhang, and Zhang (2007). Rashid, Fukumoto, Medley, Villafuerte, and Zhou (2007) suggested a special lubricant to lower the tendency to sticking of the workpieces to the electrodes thereby increasing the electrode life. The company Fronius International (2014) developed a technique called DeltaSpot using continuous tape running between the electrodes and the sheets to be joined thereby increasing the electrode life remarkably. Han (2010) reported that

frequent, light dressing of the electrodes removing pickup of aluminum increases the electrode life significantly.

Although different techniques and materials were investigated by these researchers, the influence of surface pretreatment before RSW of aluminum AA1050 and the use of mechanical pretreatment by glass blasting have not been clearly identified in any previous work. Blasting with glass beads is easy to automatize and may not cause higher costs than other surface pretreatments in mass production. Furthermore, the treatment is more environmentally friendly than chemical treatment.

The present study focuses on the influence of surface pretreatment prior to RSW of aluminum AA1050, aiming at minimizing variations in weld strength caused by the oxide layer. Mechanical pretreatment by glass blasting and chemical treatment by pickling with NaOH are compared with welding of as-received material.

2. Experimental procedure

2.1. *Workpiece material, electrodes, and welding equipment*

The experiments were conducted at the Technical University of Denmark (DTU) welding .6, 1.0, and 1.5 mm sheets of unalloyed aluminum AA1050 on a TECNA AC welding machine with specifications, as listed in Table 1. The properties and composition of the workpiece sheets determined by spectrum analysis are shown in Table 2. Samples of dimensions 16 × 115 mm were cut from delivered sheets, with the longitudinal dimension in the rolling direction. They were welded as a lap joint ready for subsequent shear-tensile testing. A hard wood fixture was used to mount the samples in good alignment with the electrodes (see Figure 1).

The electrode tips (Female Cap) were of type A according to ISO 5821-2009 and the American standard RWMA No. FF-25. They were made of zirconium–copper alloy (CuCrZr) with the following chemical composition; Cr: .7–1.2%, Zr: .06–.15%, bal. Cu. The electrodes were of dome configuration, Ø16 mm in diameter with a spherical end

Table 1. Machine specifications, TECNA AC welder.

Specifications	Values	Specifications	Values
Controller	TE-180, 16 functions	Nominal power at 50%	250 kVA
Supply voltage	380 V	Phases	1
Frequency	50 Hz	Supply pressure	6.5 bar
Max. welding current	68 kA	Electrode force per 1 bar	3.14 kN
Max. welding force	18.85 kN	Throat depth	250 mm
Max. welding power	810 kVA	Water cooling	12 l/min

Table 2. Strip material specifications.

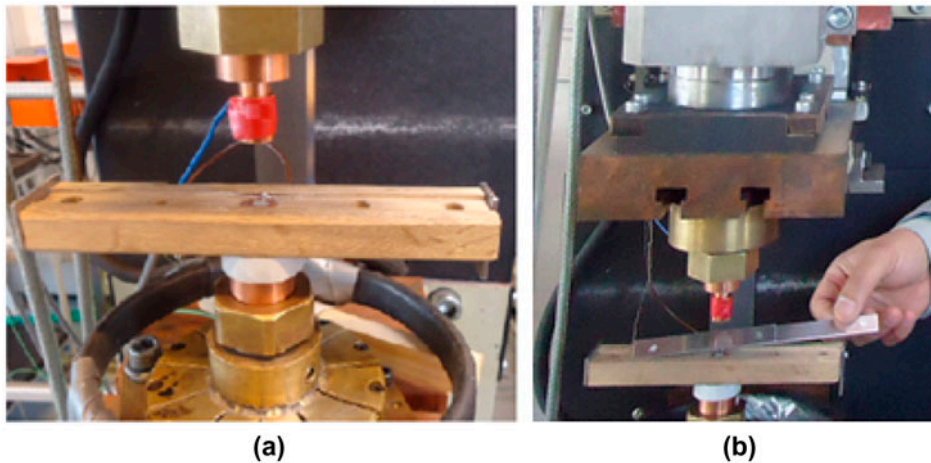| Trade name	Thickness (mm)	Tensile (MPa)	Hardness (HV)	Nominal composition (wt%)				
				Fe	Si	Mn	Others	Al
1050	.6	105	30	.255	.173	.021	.051	99.5
1050	1.0	105	30	.378	.100	.018	.004	99.5
1050	1.5	127	45	.350	.070	.010	.070	99.5

Figure 1.   Setup for welding, (a) hardwood-fixture for mounting strips, (b) removing welded strips. Pretreatment of the workpiece surfaces was done by two methods, mechanical and chemical.

surface of radius 40 mm. Close to the tip of the two electrodes, an Ø1.5-mm hole was drilled and copper wires were inserted to measure the secondary voltage over the weld.

The welding current was measured by a Rogowski coil together with a precalibrated TECNA-1430 conditioner, and a Kistler piezoelectric force transducer was used to measure the electrode load. The acquired data were treated on a PC by specially developed software in LabVIEW.

The following parameters of the RSW process were calculated for each experiment, RMS current I (A), RMS voltage U (V), welding time C (s), and the electrode force P (kN). Tensile-shear testing was carried out using a universal testing machine at a deformation rate of 2 mm/min to determine the weld strength S(N). Vickers microhardness measurements were performed with a load of 50-g testing on weld cross-sections in longitudinal direction through the diameter of the nugget at intervals of .5–1.0 mm. Macrographs and micrographs of the welds were made in light optical microscope. Moreover, high-resolution images were made in SEM, using EDS for quantitative chemical analysis.

2.2.   Shot blasting

The mechanical treatment was done by shot blasting with 100-μm glass beads. Each strip was subjected to 30 s blasting at an air pressure of 200 kPa (see Figure 2). In the main series of experiments, surface treatment was done on both sides of the strips, whereas additional experiments were performed dressing only the outer side of the strips contacting the electrodes.

2.3.   Pickling

Pickling was performed in an aqueous solution of sodium hydroxide (NaOH) (see Figure 3). During pickling of aluminum alloy strips, the surface oxides or hydroxides
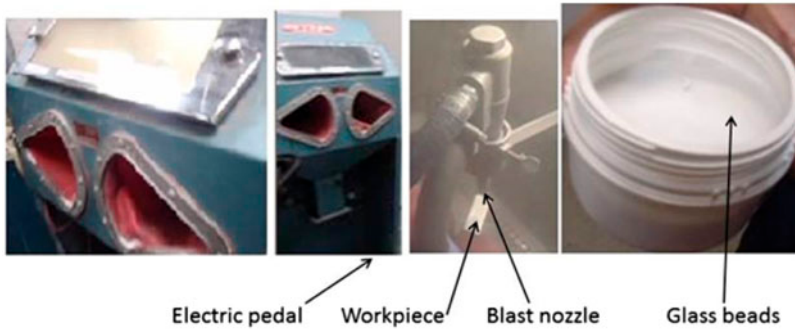
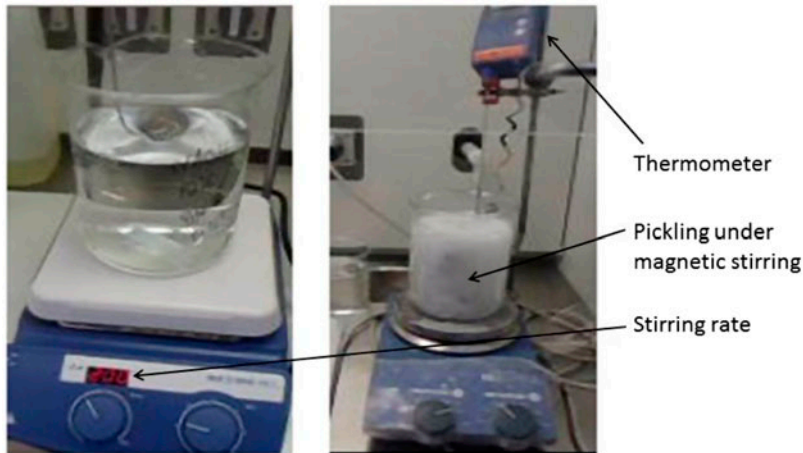Figure 2.   Glass blast surface treatment.

Figure 3.   Pickling setup.

are dissolved. The pickling rate is dependent on several variables including; (1) concentration, (2) solution temperature, (3) composition of the surface sheet, and (4) stirring rate of solution.

An aqueous solution of 60 g of NaOH per liter of water was chosen with a bath temperature of 60 °C. Magnetic stirring was done in a fume cupboard at a rate of 200 rpm. The strips were subsequently rinsed in hot water and ethanol. Preliminary experiments with 5-min pickling time resulted in severe sticking of the workpieces to the electrodes as well as expulsions between the electrodes and the strips. Due to this, pickling time was reduced to 2 min thereby minimizing these problems.

As earlier mentioned, an oxide layer is re-established on the aluminum specimens immediately after surface dressing. In order to ensure similar conditions for all experiments with surface dressing, this was carried out within 3 h before spot welding. In this way, a substantially smaller oxide layer than that of the as-received aluminum can be expected.

2.4. Plan of experiments

The experiments were planned as a general factorial with three replicates per condition (Cho et al., 2006), and the results were recorded as the average value of each condition. The welding parameters and their associated values are given in Table 3. For each of the three sheet thicknesses, three different weld currents were chosen, representing low, medium, and high welding energy. During welding, possible expulsion and sticking to the electrodes were observed and recorded.

3.   Results and discussion
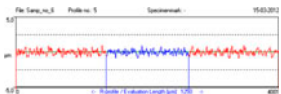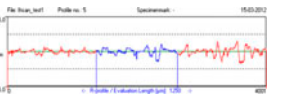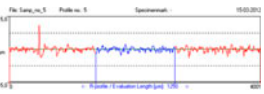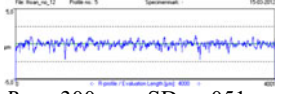
3.1. Surface roughness
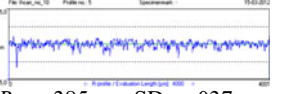
The two surface treatments were each characterized by five surface roughness measurements on three different strips. Table 4 shows the resulting R_a values. Pretreatment by glass blasting show high values of roughness, in the order of 10 times the value of the as-received surfaces. Chemical surface treatment by pickling gives a bit higher R_a values than the as-received, but the standard deviation (SD) is lower.
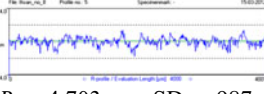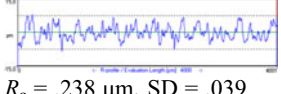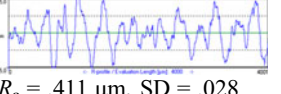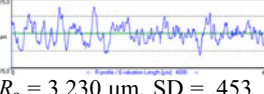
Table 3.   Experimental setup (welding parameters and values).

| Sheet (mm) | Welding energy | | | | | |
| | Low | | Medium | | High | |
	Times (cycles)	Current (kA)	Times (cycles)	Current kA	Times (cycles)	Current (kA)
.6	.04 (2)	20	.1 (5)	23	.18 (9)	26
1.0	.04 (2)	23	.1 (5)	26	.18 (9)	29
1.5	.04 (2)	26	.1 (5)	29	.18 (9)	32

Note: Electrode force 1.85–2.45 kN.

Table 4.   Surface roughness values.

Sheet (mm)	As-received	Pickling in NaOH	Glass-blast
.6	R_a = .287 μm, SD = .046	R_a = .339 μm, SD = .011	R_a = 2.650 μm, SD = .115
1.0	R_a = .300 μm, SD = .051	R_a = .385μm, SD = .037	R_a = 4.703 μm, SD = .987
1.5	R_a = .238 μm, SD = .039	R_a = .411 μm, SD = .028	R_a = 3.230 μm, SD = .453

3.2. *Electrical resistance as a function of surface condition*

In order to study the influence of surface preparation on electrical contact resistance, the total electrical resistance between the two electrodes was determined for each surface dressing condition and each sheet thickness. The resistance was calculated by dividing
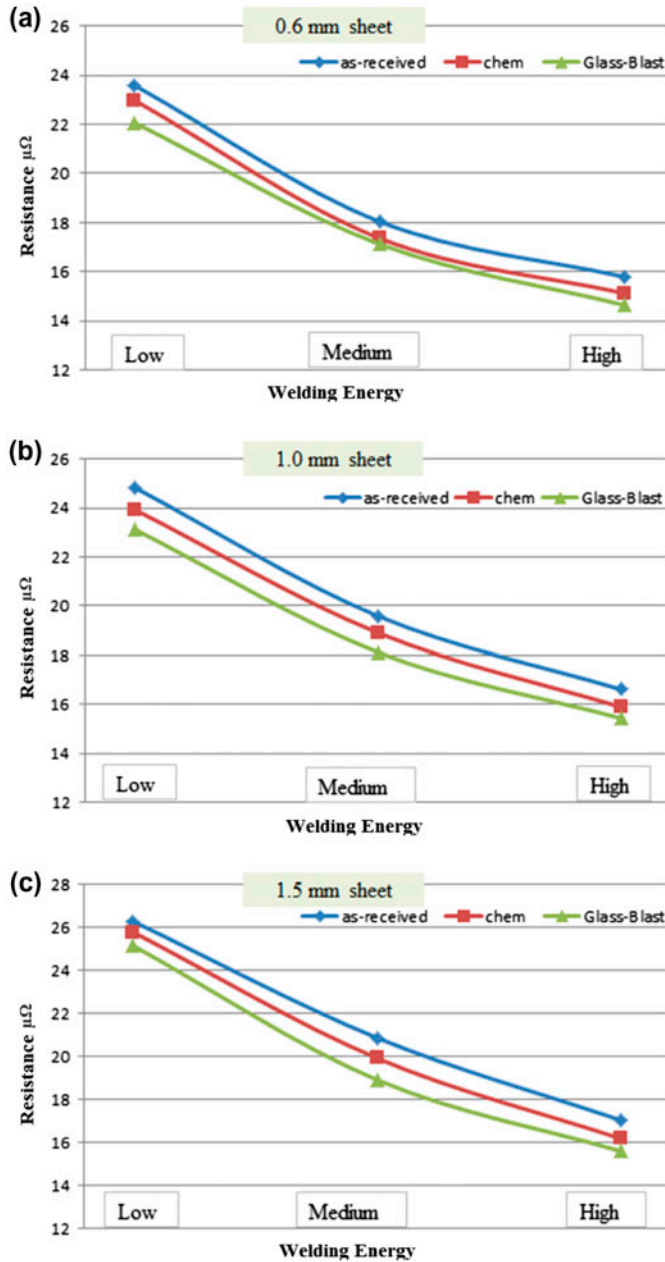

Figure 4.   Electrical resistance as a function of energy input and surface dressing for (a) .6 mm; (b) 1.0 mm; (c) 1.5 mm sheets.

the RMS voltage by the RMS current determined by sampled current and voltage data using the LabVIEW software program. The error due to induction of emf was minimized by twisting the wires, when measuring the voltage between the electrodes. Although it is the entire electric resistance between the electrodes, which is determined in this way, a comparison between the individual surface treatments gives a good idea of their influence on the accumulated contact resistance between workpieces and between workpieces and electrodes.

Figure 4 shows the total electrical resistance between the two electrodes as a function of the energy input for each surface condition and each sheet thickness. It is noticed that the as-received sheet has the highest electrical resistance for all sheet thicknesses due to the thicker oxide layer increasing the contact resistance. Medium contact resistance is obtained with chemical pickling, which lowers the contact resistance by decreasing the oxide layer thickness. The lowest electrical resistance is obtained with glass-blasted sheets, which besides removing the thick oxide film creates a rough surface causing easy breakup of the newly formed oxide layer, when the applied electrode load deforms the contacting surface asperities. It is, furthermore, noticed that the electrical resistance decreases with increasing welding energy (increased current and welding time). This might be explained by easier breakdown of the layer of oxides and contaminant film at high temperature as also observed by others (Crinon & Evans, 1998; Han et al., 2010; Song et al., 2005). Finally, a small increase in the electrical resistance is observed with increasing sheet thickness, as to be expected.

3.3.   *Microhardness tests and microstructure examinations*

Figure 5 shows the microhardness profiles for RSW of 1.0-mm sheets with the three different surface treatments. The hardness of the fusion zone FZ and the heat-affected zone (HAZ) is noted to be lower than that of the base metal for all cases due to annealing of the work-hardened base metal during welding. A few points indicate relatively low microhardness due to presence of void defects nearby, e.g. points 5 and 7 in as-received sheets and point 4 in pickled sheets.

The comparison of hardness profiles in Figure 5(d) shows the hardness in the FZ and the HAZ to be highest for welds with pretreatment by glass blasting and lowest for the case of as-received sheets. This is explained by the influence of electrical contact resistance on heat generation discussed earlier. Hardness profiles for welded 1.5-mm sheets showed the same trend.

Macrographs also showed the nugget size when welding as-received sheets to be larger than pretreated sheet surfaces. This is due to the smaller electrical contact resistance in the faying surfaces generating less heat in the latter cases. For example, the nugget sizes were 5.1, 5.0, and 4.7 mm in 1.0-mm sheets, and 7.0, 6.54, and 5.35 mm in 1.5-mm sheets for as-received, pickled, and glass-blasted sheets, respectively. The minimum nugget size was obtained by glass-blasted sheets, due to minimum electrical contact resistance.

Figure 6 shows micrographs of the 1.0-mm glass-blasted strips welded with 29-kA welding current and .1-s (five cycles) welding time. In the oval nugget region, recrystallized, small, equiaxial grains, and insoluble particles of $FeAl_3$ (black) are noticed as well as a narrow zone of columnar grains along the nugget edge nugget. Next to this zone is the HAZ, which consist of dendritic grains. Moreover, some porosities (large, black areas) are evident. No significant difference in the microstructures was found in welds between the as-received and the pretreated sheets.
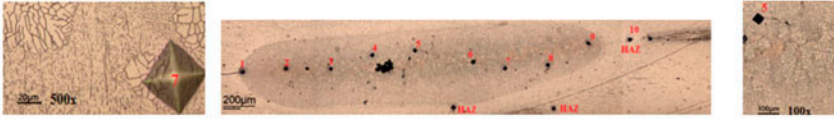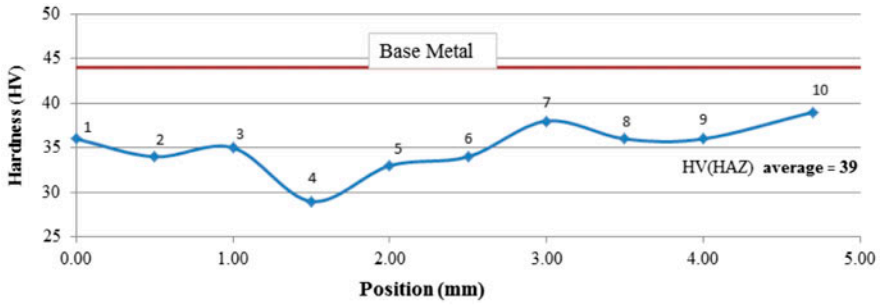
(a) Glass-blasted pretreatment surfaces
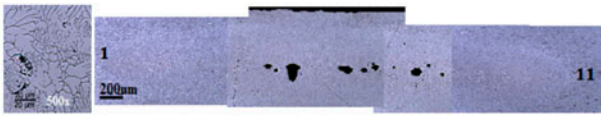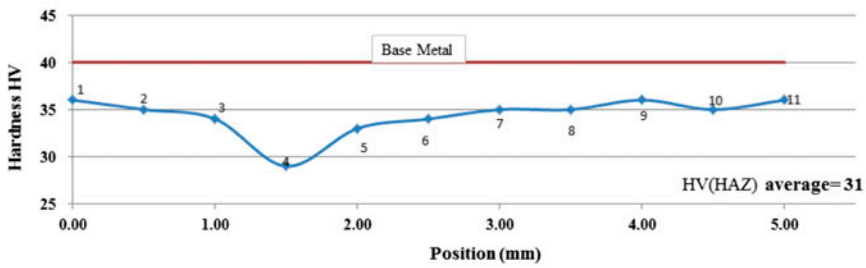
(b) Pickling in NaOH pretreatment surfaces
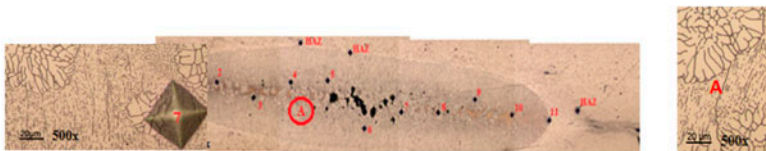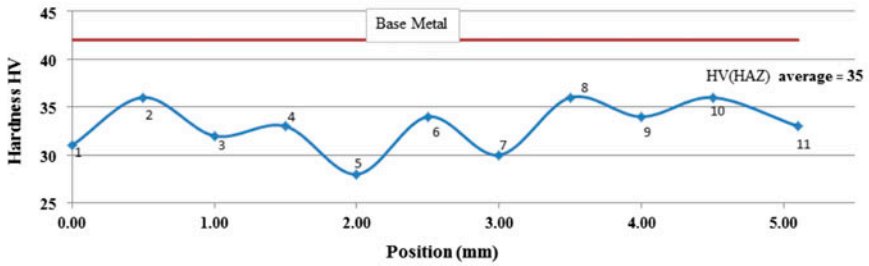
(c) As-Received sheet

Figure 5.   Microhardness profiles of 1.0-mm sheet, welding parameters 29 kA, .1 s (five cycles).

Figure 5.   (*Continued*).

Figure 6.   Micrographs of RSW of 1.0-mm sheet, welding parameters 29 kA, .1 s (five cycles).

3.4.   *Tensile-shear tests*

Tensile-shear tests of the welded joints indicate their strength and the failure mode. Figure 7 shows the strength as function of the welding energy input specified in Table 3 for the three different surface trea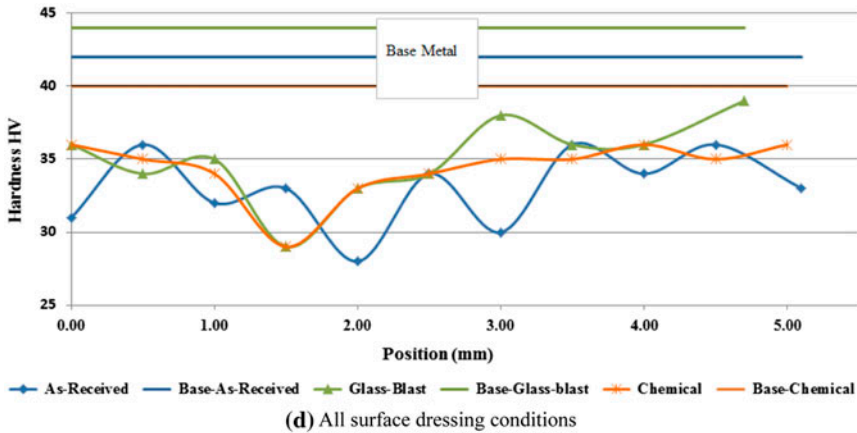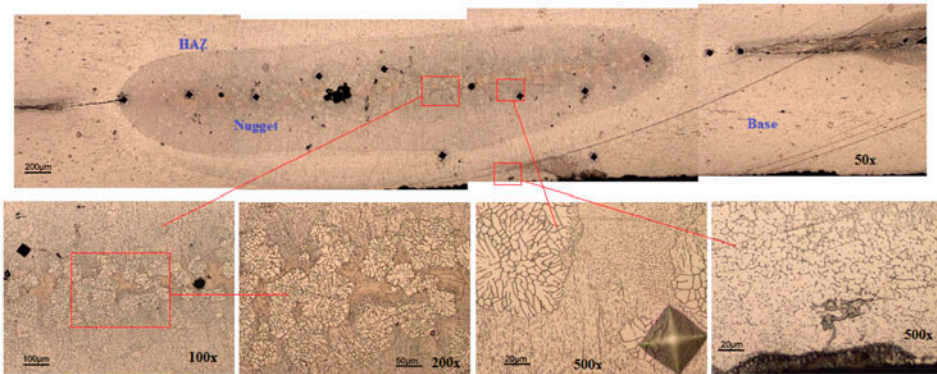tments (as-received, pickled, and glass blasted). The surface treatment is generally done on both sides of the strips, but for the case of glass blasting and medium energy input, one-sided treatment of the outer sides contacting the electrodes is also investigated. The data represented by an average value and a scatter bar are based on an average of three identical tests. It is seen that an increase in energy input increases the strength. The mode of failure was recorded in each test and classified as one of the following three types: (1) interfacial failure (nugget fracture in shear), (2) plug failure (nugget pull-out), and (3) failure in the HAZ. Failure mode 1 typically occurred at low input energy indicating insufficient heating, mode 2 at medium input energy indicating satisfactory heating, and mode 3 at high input energy indicating over-heating and softening of the region near the nugget. A few abnormal test results were observed to fall outside these types of failure. In line with other studies (Mathers, 2002;
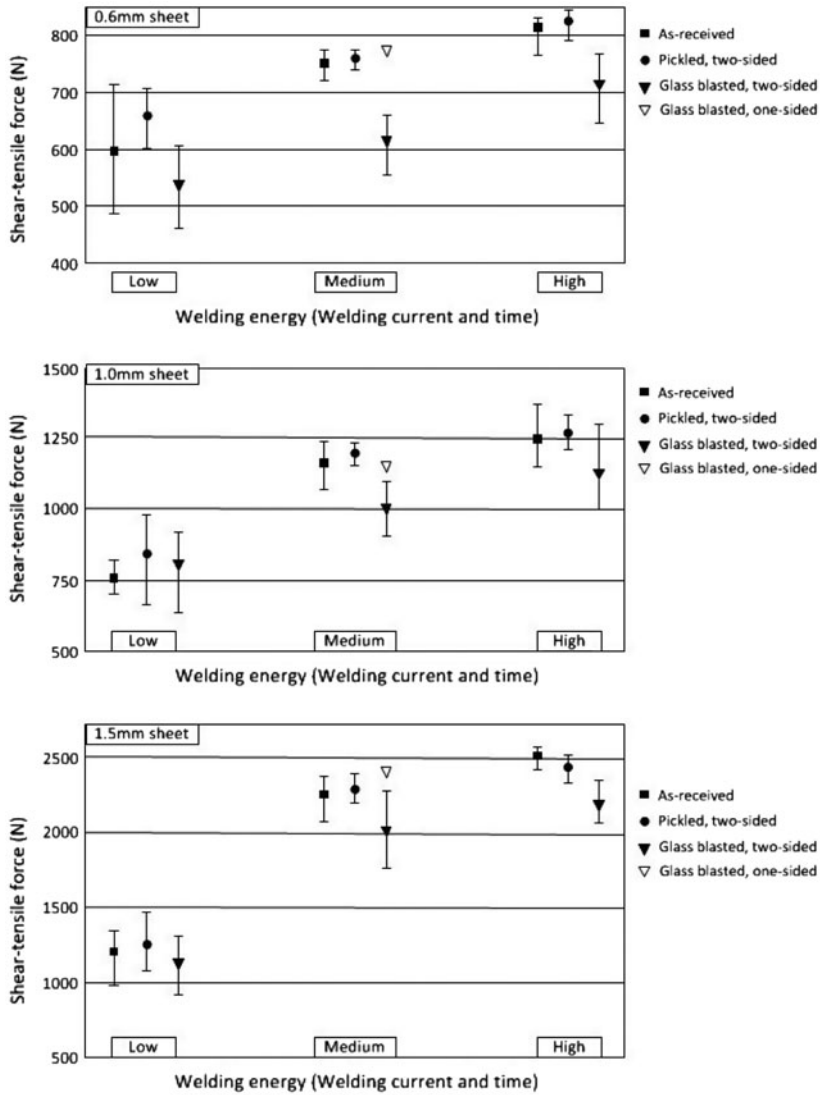
Figure 7.   Shear-tensile force vs. welding energy input for different surface treatments and sheet thicknesses.

Newton, Browne, Thornton, Boober, & Keay, 1994; Rashid, 2011; Senkara et al., 2004; Shi & Guo, 2013), expulsion and severe sticking of the workpiece to the electrodes occurred at high-energy input. Furthermore, fracture in mode 3 was usually in the form of ductile tearing around the nugget.

The scatter in weld strength is less when surface treating by pickling than for the as-received strips. Largest scatter is generally noticed for the two-sided, glass-blasted sheets, which may be attributed to the large surface roughness, low interface resistance, and difficulties in controlling this manually operated surface dressing. The treatment by pickling is also best regarding average weld strength independent of the sheet thickness.

The values for medium energy input are 760, 1193, and 2283 N for .6, 1.0, and 1.5-mm sheets, respectively. The lowest strength is obtained for the glass-blasted sheets due to the lowest values of electric contact resistance; see Figure 4, which leads to small nugget size. The values for medium heat input are 616, 1008, and 2020 N for .6, 1.0, and 1.5-mm, respectively. The low electrical contact resistance of the glass-blasted, rough surfaces may be attributed to easier breaking up of the oxide layer as also observed by other authors (Dzekster & Ismailov, 1990; Han et al., 2010; Song et al., 2005).

If only the surfaces contacting the electrodes are glass blasted leaving the faying surfaces untreated, a significant increase in strength occurs, i.e. 775, 1147, and 2408 N for .6, 1.0, and 1.5-mm sheet thickness, respectively, for medium-energy input. The reason for this is higher heat generation due to higher electrical contact resistance at the faying surfaces. This treatment is recommendable, since it also ensures less sticking to the electrodes, and thus increased electrode life. The fact that pickling improves weld quality as regards level and consistency compared to the as-received surface condition even if the surface roughness is similar indicates that the latter is not of overriding importance controlling the electric contact resistance although increasing roughness may facilitate breakdown of the oxide layer. The main importance is the thickness of the oxide layer as also stated by other researchers (Patrick et al., 1984; Song et al., 2005; Sun, 1982).

3.5. SEM and EDS examinations

Micrographs were also made in SEM to study microstructure and surface profile and carry out high-resolution mapping determining chemical composition of areas of special interest by X-ray spectroscopy (EDS). When welding as-received sheet (with thick oxide layers), considerable indentation into the aluminum sheets was observed, as well as rapid degradation of the electrodes. This was due to pitting of the electrode surfaces and dissolving or diffusion of copper into the aluminum workpiece material and vice versa (see Figure 8(a)).
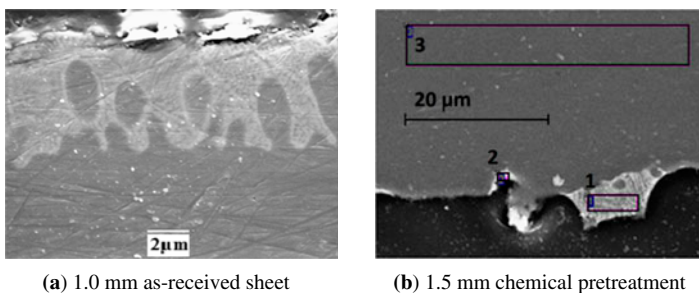
(a) 1.0 mm as-received sheet   (b) 1.5 mm chemical pretreatment

	Al	O	Cu	Total
1	69.4	1.0		100
2	66.5	2.2		100
3	100			100
Max.	100	2.2	31.3	
Min.	66.5	1.0	29.6	

(c) EDS analysis

Figure 8.   SEM images RSW and measured composition referring to Figure 5(b).
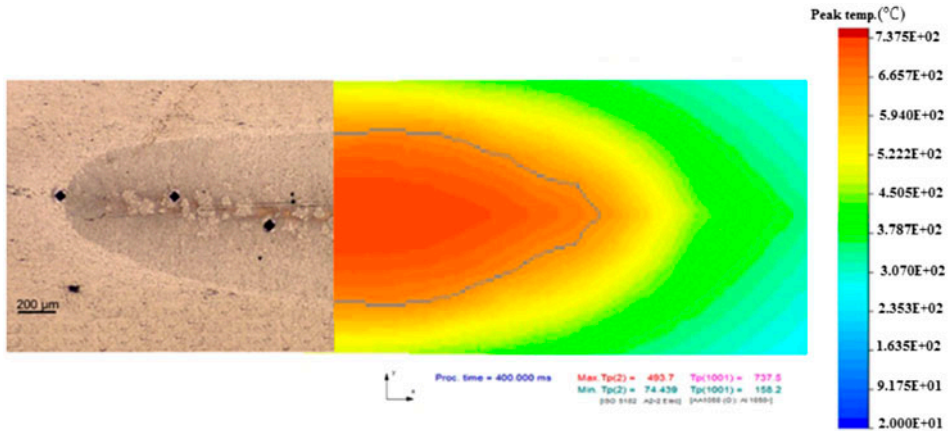
Figure 9.   Comparison of experimental and predicted nugget shape.

Welding of pretreated sheets showed less indentation and dissolving of electrode material in the workpiece due to a thinner oxide layer causing less heating (Figure 8(b)). The reason for a few defects in this case may be pitting of the electrode surface. The white colored areas in the SEM images indicate the presence of oxide as well as dissolving of copper into the workpiece, as shown in the EDS analysis table in Figure 8(c).

3.6.   Numerical simulation

The commercial finite element program SORPAS® developed especially for resistance welding (SWANTEC Software & Engineering ApS. SORPAS®) was used in the present work. It combines mechanical, electrical, thermal, and metallurgical models analyzing the development of heat and distributions of current, voltage, temperature, stresses, and strains (Bay & Zhang, 2007; Zhang, 2003). Using a new feature called Weld Schedule Specifications optimized weld current, electrode force, welding time, and holding time were calculated, see Table 5, for welding of as-received as well as surface-dressed sheet adjusting the input value of the electrical resistance at 20 °C in the materials database of the program to lower value in case of surface dressing according to Figure 4. It is clearly noted that especially the proposed welding current for the pretreated surfaces is lower than that for as-received sheets.

Figure 9 shows a comparison between predicted and actual weld nugget with as-received strip surface, in 1.0-mm sheet for 27-kA welding current and .1-s five cycles welding time. It is noticed that the nugget shape is rather well predicted.

Table 5.   WSS of weld planning optimization SORPAS.

Sheet	As-Received (mm)			Pretreatment (mm)		
	0.6	1.0	1.5	0.6	1.0	1.5
Welding Current (kA)	23.9	26.27	31.64	22.87	24.58	27.26
Welding Time (cycles)	2	4	5	2	4	4
Electrode Force (kN)	1.16	1.44	1.78	1.04	1.44	1.49

4.   Conclusions

The experiments showed that consistency in weld quality is improved when the oxide layer of the as-received aluminum surfaces is properly removed. However, the resistance of an oxide layer is beneficial at the interface between the faying surfaces in order to increase local heating to form the weld nugget, whereas the resistance at the contact between electrodes and workpiece should be as low as possible to avoid sticking and poor electrode life. The most significant conclusions drawn from this experimental work are as follows:

(1) The surface condition of the aluminum sheets has significant influence on the weldability and the electrode lifetime.

(2) The highest value of electrical contact resistance is obtained with as-received sheet due to a thicker oxide layer.

(3) Pretreatment by pickling in 60 °C NaOH gives highest weld strength and lowest scatter. Optimum pickling time is 2 min.

(4) Lowest contact resistance is obtained by glass blasting, which besides removing the original oxide film provides a rough surface decreasing the contact resistance due to breakdown of the oxide layer by asperity deformation.

(5) One-sided surface treatment by glass blasting of the surfaces contacting the electrodes is favorable leading to less electrode sticking, and thus increased electrode life and furthermore better weld strength than two-sided glass blasting.

(6) The microhardness in the FZ and HAZ is lower than in the base metal for all cases due to annealing of the as-received, workhardened material.

(7) SEM and EDS examinations confirm the presence of copper (electrode material) in the welded aluminum strips especially when welding as-received sheet indicating degradation of the electrodes due to dissolving and diffusion, which may furthermore cause pitting and accelerated electrode wear due to the pitting on the surface of the electrodes.

(8) Numerical simulation with SORPAS® gives good prediction of appropriate welding parameters and nugget size.

References

Bay, N., & Zhang, W. (2007, May). Thermomechanical modelling of resistance welding. *Proceedings of International Conference on Computational Methods for Coupled Problems in Science and Engineering* (162–165). Ibiza, Spain.

Boomer, D. R., Hunter, J. A., & Castle, D. R. (2003). *A new approach for robust high-productivity resistance spot welding of aluminum* (SAE Technical Paper -01-0575).

Brown, D. J., Newton, C. J., & Boomer, D. (1995). Optimization and validation of a model to predict the spot weldability parameter lobes for aluminum automotive body sheet. Advanced Technologies & Processes. In *Proceedings of International Body Engineering Conference, IBEC* (pp. 100–106).

Cho, Y., Li, W., & Hu, S. J. (2006). Design of experiment analysis and weld lobe estimation for aluminum resistance spot welding. *AWS Welding Journal, 85*, 45s–51s.

Crinon, E., & Evans, J. T. (1998). The effect of surface roughness, oxide film thickness and interfacial sliding on the electrical contact resistance of aluminum. *Material Science and Engineering Journal, A242*, 121–128.

Dzekster, N. N., & Ismailov, V. V. (1990). Some methods for Improving Aluminum Contacts. In *Proceedings of 36th Annual Holm Conference on Electrical Contacts* (pp. 518–520). Chicago, IL, Illinois Institute of Technology.

Fronius International. (2014, September). Retrieved from http://www.fronius.com/cps/rde/xchg/SID-3AC27A9B-F495FC44/fronius_international/hs.xsl/79_33390_ENG_HTML.htm#.VBmeZaPU-70

Han, L. (2010, September 22–24). Development of RSW Al for LWV manufacture. In *Proceedings of the 6th International Seminar on Advances in Resistance Welding* (pp. 55–70). Hamburg.

Han, L., Thornton, M., Boomer, D., & Shergold, M. (2010). Effect of aluminium sheet surface conditions on feasibility and quality of resistance spot welding. *Journal of Materials Processing Technology, 210*, 1076–1082.

Kim, D. C., Park, H. J., Hwang, I. S., & Kang, M. J. (2009). RSW of aluminum alloy sheet 5J32 Using SCR type and inverter type power supplies. *International Scientific Journal, 38*, 55–60.

Li, Z., Hao, C., Zhang, J., & Zhang, H. (2007, April). Effects of sheet surface conditions on electrode life in resistance welding aluminum. *Welding Journal*, 81–89.

Mathers, G. (2002). *The welding of aluminum and its alloys*. Cambridge: Woodhead.

Newton, C. J., Browne, D. J., Thornton, M. C., Boober, D. R., & Keay, B. F. (1994). *The fundamental of resistance spot welding aluminum*. Sheet Metal Conference VI; Paper E2.

Patrick, E. P., Auhl, J. R., & Sun, T. S. (1984). *Understanding the process mechanism is key to reliable resistance spot welding aluminum auto body components* (SAE Technical Paper 840291).

Pedersen, K. R. (2010). *Resistance welding of aluminum alloys* (Master thesis). Department of Mechanical Engineering, Technical University of Denmark.

Pickering, E. R., & Hart, C. J. (1994). *Optimizing resistance spot welding on aluminium alloy 6111 auto body sheet* (SAE Technical Paper, 940662).

Rashid, M. (2011). Some tribological influences on the electrode-worksheet interface during resistance spot welding of aluminum alloys. *Journal of Materials Engineering and Performance, 20*, 456–462.

Rashid, B. M., Fukumoto, S., Medley, J. B., Villafuerte, J., & Zhou, Y. (2007, March). Influence of lubricants on electrode life in resistance spot welding of aluminum alloys. *Welding Research*, 62–70.

Resistance Welding Manual. (2003). Bridgeport, NJ: RWMA Resistance Welding Manufacturers Association.

Rönnhult, T., Rilby, U., & Olefjord, I. (1980). The surface state and weldability of aluminium alloys. *Materials Science and Engineering, 42*, 329–336.

Senkara, J., Zhang, H., & Hu, S. J. (2004). Expulsion prediction in resistance spot welding. *AWS, Welding Journal, 83*, 123s–132s.

Shi, Y., & Guo, H. (2013). Fatigue performance and fatigue damage parameter estimation of spot welded joints of aluminium alloys 6111-T4 and 5754. *Fatigue & Fracture of Engineering Materials & Structures, 36*, 1081–1090.

Song, Q., Zhang, W., & Bay, N. (2005). An experimental study determines the electrical contact resistance in resistance welding. *AWS Welding Journal, 84*, 73s–76s.

Spinella, D. J., Brockenbrough, J. R., & Fridy, J. M. (2005). Trends in aluminum resistance spot welding for the auto industry. *AWS Welding Journal, 84*, 34–41.

Sun, M. A. (2003). *Fundamental study of contact resistance behavior in RSW aluminum* (PhD dissertation). School of The Ohio State University, Ohio State University.

Sun, T. S. (1982). *Electrode deterioration mechanisms in resistance spot welding of aluminum* (AlCOA Internal Report No. 53-82-3).

SWANTEC Software and Engineering ApS. SORPAS® (Version 10.6). Retrieved from http://www.swantec.com

Thornton, M. C., Newton, C. J., Keay, B. F. P., Sheasby, P. G., & Evans, J. T. (1997). Some surface factors that affect the spot welding of aluminium. *Transactions of Institute of Metal Finishing, 75*, 165–170.

Wheeler, M. J., Sheasby, P. G., & Kewley, D. (1987). *Aluminum structured vehicle technology. A comprehensive approach to vehicle design and manufacturing aluminum* (SAE Technical Paper 870146).

Zhang, H., & Senkara, J. (2012). *Resistance welding – Fundamentals and applications* (2nd ed.). Boca Raton, FL: Taylor & Francis Group, LLC.

Zhang, W. (2003). Design and implementation of software for resistance welding process simulations. Welding & Joining, SP-1766, SAE. In *World Congress* (pp. 105–113). Detroit, MI, USA.

Zheng, Z. T., Shan, P., Hu, S. S., & Luo, Z. (2006). Resistance spot welding of aluminum alloy with great resistance medium. *Transactions of the China Welding Institution, 27*, 5–8.